J. Fluid Mech. (1976), *vol.* 76, *part* 2, *pp.* 289–306
Printed in Great Britain

On the stability of the Stewartson layer

By KIYOSHI HASHIMOTO

Department of Aeronautical Engineering, Faculty of Engineering,
Kyoto University, Kyoto, Japan

(Received 29 December 1975)

The stability of the Stewartson layer in a rotating incompressible fluid is investigated within the framework of a linear theory. The boundary-layer structure of the shear layer is correctly taken into account and the effect of viscous dissipation on the disturbance is included in the governing equations. The growth rate ω_i of the disturbance is given as a function of the unified parameter $m\,Ro/(\gamma E^{\frac{1}{2}})$, where m, an integer, is the azimuthal component of the wavenumber vector, γ the radius of the layer, Ro the Rossby number and E the Ekman number. Instability occurs when $m\,Ro/(\gamma E^{\frac{1}{2}}) > 9{\cdot}5$. The time evolution of a growing disturbance is given schematically. Comparison of our results with the experiments by Hide & Titman shows good agreement.

1. Introduction

Recently, Hide & Titman (1967) performed an elaborate experiment on the stability of a shear layer in a rotating liquid. They produced the shear layer by inserting a circular disk into a rotating flow in a cylindrical tank. The disk rotated concentrically with the tank, but with a different angular velocity (see figure 1). When the relative difference between the angular velocities of the tank and the disk was smaller than a certain critical value, they observed an axisymmetric steady configuration. When this critical value was exceeded, however, the free shear layer (the Stewartson layer) exhibited an azimuthal distortion. As in the case of the Taylor–Proudman column, the distortion did not depend on the axial co-ordinate. When the disk rotated faster than the tank, this distortion had a regular wavy flow pattern with azimuthal wavenumber m which moved with approximately the same angular velocity as the tank. The wavenumber m decreased as the relative difference in angular velocities increased. In the opposite case in which the disk rotated slower than the tank, distortion occurred at the same absolute value of the relative difference in angular velocities. The flow pattern, however, differed from that of the wavy motion, being in the form of an off-axis ellipse. Hide & Tidman gave detailed tables of experimental data: the apparatus, the configuration, the Ekman number, the Rossby number and the wavenumber m at which the instability set in.

Corresponding to this experiment, Busse (1968) and Siegmann (1974) have performed linearized analyses of shear-layer instability in a rotating fluid. Siegmann also studied nonlinear effects on the basis of Stuart's method. The shear layers they considered were, however, much thicker than the Stewartson

(1957) shear layer. This led to the neglect of the effect of dissipation on the disturbance, and to oversimplification of the basic flow.

In this paper, we study the effect of lateral dissipation on the linear stability of the Stewartson layer. For this purpose, we take the exact velocity distribution in the Stewartson layer as our basic flow, and apply Hunter's (1967) boundary-layer method of solution to the viscous equation of the disturbances.

The most interesting aspect of our results is a similarity law by which parameters in the dispersion equation are combined into the single parameter $m\,Ro/\gamma E^{\frac{1}{2}}$, where Ro is the Rossby number, E the Ekman number and γ is the non-dimensional radius of the Stewartson layer. Instability occurs when this parameter exceeds 9·5. As is shown in figure 5 in §6, predictions based on this result compare well with Hide & Titman's experiments. Because of the linearization, however, we failed to predict the asymmetry of the flow with respect to the sign of the relative difference between the angular velocities of the disk and the tank.

In §2 the basic equations are given. In §3 they are solved using Hunter's boundary-layer method of solution and under an assumption about the behaviour of the inviscid solution. In §4 this assumption is examined to prove the self-consistency of our method. In §5 the energy balance for the disturbances is discussed. Finally, in §6, numerical results and a discussion are given.

2. Basic equations and main flow

Two parallel infinite flat plates rotate around the same vertical axis. The distance between the plates is $2H$. There are narrow annular gaps at a radius R in both plates. The inner parts of the plates, inside these gaps, rotate with the same angular velocity $\Omega-\frac{1}{2}\Delta\Omega$, and the outer parts with angular velocity $\Omega+\frac{1}{2}\Delta\Omega$. The space between the plates is filled by viscous incompressible fluid. The situation is shown schematically in figure 1. As was discussed by Stewartson (1957), the fluid between the inner and outer parts of the plates respectively rotates rigidly with the corresponding parts of the plates. Double Stewartson layers of thicknesses $E^{\frac{1}{3}}$ and $E^{\frac{1}{4}}$ bridge the velocity discontinuity between the inner and outer region. Our problem is to study the stability of this shear layer.

Let us introduce a system of cylindrical co-ordinates (r, θ, z) which rotates with angular velocity Ω. The origin of the co-ordinates is the point on the rotation axis midway between the plates. Position vectors are non-dimensionalized by H, velocities by $\frac{1}{2}H\Delta\Omega$ and the perturbed pressure by $\rho HR\Omega\Delta\Omega$, where ρ is the density. The dimensionless forms of the linearized basic equations governing small disturbances are

$$\nabla.\mathbf{q} = 0, \tag{2.1}$$

$$E^{\frac{1}{2}}\partial\mathbf{q}/\partial t + Ro\{(\mathbf{U}.\nabla)\mathbf{q} + (\mathbf{q}.\nabla)\mathbf{U}\} + \mathbf{k}\times\mathbf{q} = -\nabla p + \tfrac{1}{2}E\Delta\mathbf{q}, \tag{2.2}$$

where $Ro = R\Delta\Omega/4\Omega H$, the Rossby number, and $E = \nu/H^2\Omega$, the Ekman number. In these equations, $\mathbf{U}[=(U, V, W)]$ is the velocity of the basic flow, $\mathbf{q}[=(u, v, w)]$ the perturbation velocity, $\mathbf{k}$ a unit vector along the axis of rotation, p the pressure and ν the kinematic viscosity. We assume that E is much

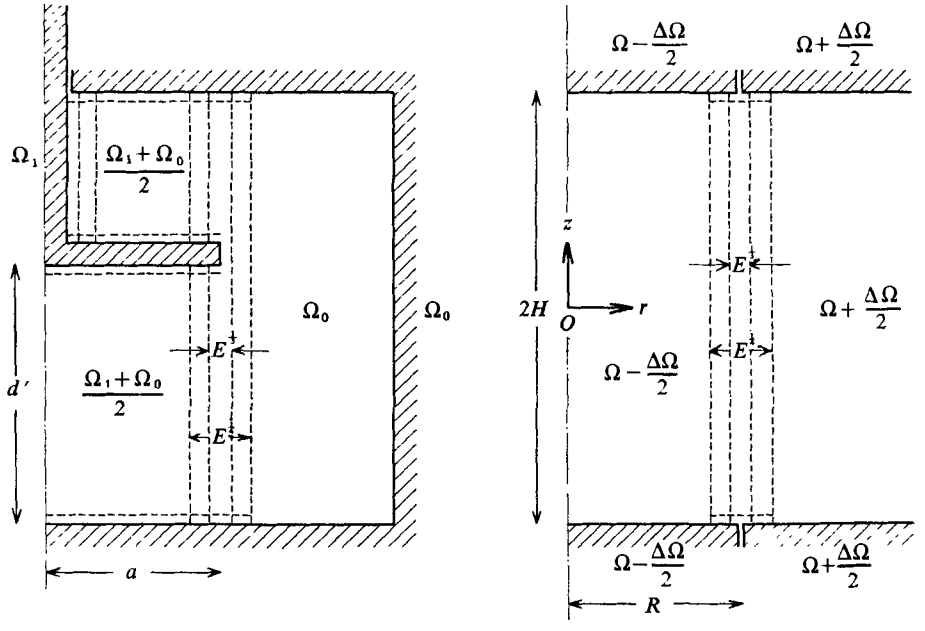

FIGURE 1. The schematic representation of the configuration in (*a*) Hide & Titman's experiment and (*b*) in the present paper.

smaller than unity and that Ro is of order $E^{\frac{1}{2}}$. The parameter range of Hide & Titman's experiment is consistent with these assumptions. We have non-dimensionalized the time by $2\Omega^{-1}E^{\frac{1}{2}}$. This reflects the fact that the phase velocity of the disturbance observed in the above experiment was of the same order of magnitude as the azimuthal component of the basic flow.

The flow field is divided into three regions; the $E^{\frac{1}{3}}$-layer, the $E^{\frac{1}{4}}$-layer and the inviscid region. The inner part of the $E^{\frac{1}{4}}$-layer and the outer part of the inviscid region are separated by the $E^{\frac{1}{3}}$-layer. The approximate versions of (2.1) and (2.2) in each region are solved subject to Ekman's compatibility conditions on the plates and matching conditions between different regions. Because of the homogeneity of these conditions, we arrive at a dispersion equation by this procedure. The Ekman compatibility conditions on the plates (Greenspan 1968, p. 46) are

$$w = \mp \frac{E^{\frac{1}{2}}}{2r}\left\{\frac{\partial(rv)}{\partial r} - \frac{\partial u}{\partial \theta}\right\} \quad \text{at} \quad z = \pm 1. \tag{2.3}$$

As for the radial boundary conditions, it is required that the solutions be finite at $r = 0$ and ∞ and that the solutions and their derivatives be continuous across the boundaries between the regions.

The basic flow fields have been studied by many authors (see, for example, Stewartson 1957; Hunter 1967; Hashimoto 1975). Their results give

$$U = 0, \quad V = \mp r/\gamma, \quad W = 0 \tag{2.4}$$

in the inviscid region,

$$U = O(E^{\frac{1}{3}}), \quad V = \mp 1 \pm e^{\pm\eta} + O(E^{\frac{1}{3}}), \quad W = O(E^{\frac{1}{4}}) \tag{2.5}$$

in the $E^{\frac{1}{4}}$-layer and

$$U = O(E^{\frac{7}{12}}), \quad V = E^{\frac{1}{12}}\xi + O(E^{\frac{1}{3}}), \quad W = O(E^{\frac{1}{4}}) \tag{2.6}$$

in the $E^{\frac{1}{3}}$-layer, where the upper and lower signs refer to the inner and outer parts of a region respectively, $\gamma\,(=R/H)$ is the non-dimensional radius of the free shear layer, $\eta = E^{-\frac{1}{4}}(r-\gamma)$ and $\xi = E^{-\frac{1}{3}}(r-\gamma)$. For the sake of definiteness, we assume implicitly that the inner parts of the flat plates rotate more slowly than the outer parts. The opposite case can be treated changing the sign of Ro.

3. The Stewartson layer

The Stewartson layer is composed of two shear layers whose thicknesses are of order $E^{\frac{1}{4}}$ and $E^{\frac{1}{3}}$, respectively. On the basis of the matching between these regions, we expand physical quantities in power of $E^{\frac{1}{12}}$:

$$f = f_0 + E^{\frac{1}{12}}f_1 + E^{\frac{1}{3}}f_2 + E^{\frac{1}{4}}f_3 + E^{\frac{1}{3}}f_4 + E^{\frac{5}{12}}f_5 + E^{\frac{1}{2}}f_6 + \ldots, \tag{3.1}$$

where f is an arbitrary physical quantity. Substitution of (3.1) into (2.1) and (2.2) leads to the approximate equations in each region.

The $E^{\frac{1}{4}}$-layer

We use carets to denote variables in the $E^{\frac{1}{4}}$-layer and introduce a stretched variable η defined by $\eta \equiv (r-\gamma)E^{-\frac{1}{4}}$. The equations for $\hat{u}_j$ and $\hat{p}_j$ ($j = 0, 1$ and 2) are

$$\frac{\partial \hat{u}_j}{\partial \eta} = 0, \quad 0 = \frac{\partial \hat{p}_j}{\partial \eta}, \quad \hat{u}_j = -\frac{1}{\gamma}\frac{\partial \hat{p}_j}{\partial \theta}, \quad 0 = \frac{\partial \hat{p}_j}{\partial z}. \tag{3.2}$$

Let us assume that $\hat{u}_j$ and $\hat{p}_j$ tend to zero as $|\eta| \to \infty$. This assumption is related to the behaviour of the inviscid flow and will be proved to be self-consistent in §4. This gives us $\hat{u}_j = \hat{p}_j = 0$ ($j = 0$, 1 and 2). For $\hat{u}_3$, $\hat{v}_0$, $\hat{w}_0$ and $\hat{p}_3$ we have

$$\frac{\partial \hat{u}_3}{\partial \eta} + \frac{1}{\gamma}\frac{\partial \hat{v}_0}{2\theta} + \frac{\partial \hat{w}_0}{\partial z} = 0, \tag{3.3}$$

$$\hat{v}_0 = \partial \hat{p}_3/\partial \eta, \tag{3.4}$$

$$\hat{u}_3 = -\gamma^{-1}\partial \hat{p}_3/\partial \theta, \tag{3.5}$$

$$0 = \partial \hat{p}_3/\partial z, \tag{3.6}$$

where we have used the fact that $\hat{u}_0 = \hat{p}_0 = 0$. From (3.6), (3.4) and (3.5), $\hat{p}_3$, $\hat{v}_0$ and $\hat{u}_3$ are independent of z. Combining this fact with Ekman's compatibility conditions and (3.3), we obtain $\hat{w}_0 = 0$. Using these results we get the equations for $\hat{u}_6$, $\hat{v}_3$, $\hat{w}_3$ and $\hat{p}_6$:

$$\frac{\partial \hat{u}_6}{\partial \eta} + \frac{\hat{u}_3}{\gamma} + \frac{1}{\gamma}\frac{\partial \hat{v}_3}{\partial \theta} - \frac{\eta}{\gamma^2}\frac{\partial \hat{v}_0}{\partial \theta} + \frac{\partial \hat{w}_3}{\partial z} = 0, \tag{3.7}$$

$$\hat{v}_3 = \partial \hat{p}_6/\partial \eta, \tag{3.8}$$

$$\frac{\partial \hat{v}_0}{\partial t}+\beta\frac{d\hat{V}_0}{d\eta}\hat{u}_3+\frac{\beta}{\gamma}\hat{V}_0\frac{\partial \hat{v}_0}{\partial\theta}+\hat{u}_6=-\frac{1}{\gamma}\frac{\partial \hat{p}_6}{\partial\theta}+\frac{\eta}{\gamma^2}\frac{\partial \hat{p}_3}{\partial\theta}+\frac{1}{2}\frac{\partial^2\hat{v}_0}{\partial\eta^2}, \tag{3.9}$$

$$0=\partial\hat{p}_6/\partial z, \tag{3.10}$$

where $\beta\equiv RoE^{-\frac{1}{2}}$. The corresponding Ekman compatibility conditions are

$$\hat{w}_3=\pm\tfrac{1}{2}\partial\hat{v}_0/\partial\eta \quad \text{at} \quad z=\pm 1. \tag{3.11}$$

Inspection of (3.9), (3.8) and (3.10) shows us that $\hat{u}_6$ is independent of z. Thus (3.7) can be integrated with respect to z subject to (3.11). The result of this integration and (3.4), (3.5), (3.8) and (3.9) enable us to eliminate $\hat{v}_0$, $\hat{u}_3$, $\hat{v}_3$ and $\hat{p}_6$ to obtain a single equation for $\hat{p}_3$:

$$\frac{1}{2}\frac{\partial^4\hat{p}_3}{\partial\eta^4}-\frac{\partial^3\hat{p}_3}{\partial\eta^2\partial t}-\frac{1}{2}\frac{\partial^2\hat{p}_3}{\partial\eta^2}-\frac{\beta}{\gamma}\hat{V}_0\frac{\partial^3\hat{p}_3}{\partial\theta\partial\eta^2}+\frac{\beta}{\gamma}\frac{d^2\hat{V}_0}{d\eta^2}\frac{\partial\hat{p}_3}{\partial\theta}=0. \tag{3.12}$$

If we assume a solution of the form

$$\hat{p}_3=\mathrm{Re}[\hat{\chi}_3(\eta)\exp\{i(m\theta-\omega t)\}], \tag{3.13}$$

we obtain

$$\frac{d^4\hat{\chi}_3}{d\eta^4}+2\left(i\omega-\frac{1}{2}-im\frac{\beta}{\gamma}\hat{V}_0\right)\frac{d^2\hat{\chi}_3}{d\eta^2}+2im\frac{\beta}{\gamma}\frac{d^2\hat{V}_0}{d\eta^2}\hat{\chi}_3=0. \tag{3.14}$$

The asymptotic behaviour of the four solutions of (3.14) as $|\eta|\to\infty$ can be estimated on the basis of the fact that $|\hat{V}_0|\to 1$ in the limit:

$$\hat{\chi}_3\to e^{\mu\eta},\quad e^{-\mu\eta},\quad \eta \quad \text{or} \quad \text{constant}, \tag{3.15}$$

where $$-\mu^2=2(i\omega-\tfrac{1}{2}\pm im\beta/\gamma), \quad \mathrm{Re}\,\mu>0 \quad \text{when} \quad \eta\lesssim 0. \tag{3.16), (3.17}$$

By our assumption after (3.2), the solution which grows exponentially and the solution proportional to η in the limit are discarded. The two solutions retained are

$$1-\frac{2im\beta/\gamma}{1-\mu^2}e^{\eta} \tag{3.18}$$

and

$$e^{\mu\eta}\left\{1+\sum_{k=1}^{\infty}e^{k\eta}\left(2im\frac{\beta}{\gamma}\right)^k\frac{\mu(\mu-1)}{(\mu+k-1)(\mu+k)}\prod_{n=1}^{k}\frac{1}{n(2\mu+n)}\right\}. \tag{3.19}$$

The above gives the solutions for $\eta<0$, for which μ is defined by (3.16). The solutions for $\eta>0$ are obtained by changing the signs of β and η and using the definition (3.17) for μ.

The $E^{\frac{1}{3}}$-layer

We use tildes over letters to denote physical quantities in the $E^{\frac{1}{3}}$-layer and introduce a stretched variable ξ defined by $\xi\equiv(r-\gamma)E^{-\frac{1}{3}}$. The equations for $\tilde{u}_j$ and $\tilde{p}_j$ ($j=0$, 1 and 2) are

$$\frac{\partial\tilde{u}_j}{\partial\xi}=0,\quad \frac{\partial\tilde{p}_j}{\partial\xi}=0,\quad \tilde{u}_j=-\frac{1}{\gamma}\frac{\partial\tilde{p}_j}{\partial\theta},\quad \frac{\partial\tilde{p}_j}{\partial z}=0. \tag{3.20}$$

Because $\hat{u}_0=\hat{u}_1=\hat{u}_2=\hat{p}_0=\hat{p}_1=\hat{p}_2=0$, we have $\tilde{u}_j=\tilde{p}_j=0$ for $j=0$, 1 and 2. Equations (3.20) also hold for $\tilde{u}_3$ and $\tilde{p}_3$ because $\tilde{u}_0=0$. Thus $\tilde{u}_3$ is independent of ξ and we obtain the following matching condition:

$$[\hat{u}_3]_-=[\tilde{u}_3]_+, \tag{3.21}$$

where $[\hat{f}]_+ = \lim_{\eta \to +0} \hat{f}(\eta)$ and $[\hat{f}]_- = \lim_{\eta \to -0} \hat{f}(\eta)$. For $\tilde{u}_{j+4}$, $\tilde{v}_j$, $\tilde{w}_j$ and $\tilde{p}_{j+4}$ ($j = 0$ and 1) we have

$$\frac{\partial \tilde{u}_{j+4}}{\partial \xi} + \frac{1}{\gamma} \frac{\partial \tilde{v}_j}{\partial \theta} + \frac{\partial \tilde{w}_j}{\partial z} = 0, \tag{3.22}$$

$$\tilde{v}_j = \partial \tilde{p}_{j+4} / \partial \xi, \tag{3.23}$$

$$\tilde{u}_{j+4} = -\frac{1}{\gamma} \frac{\partial \tilde{p}_{j+4}}{\partial \theta} + \frac{1}{2} \frac{\partial^2 \tilde{v}_j}{\partial \xi^2}, \tag{3.24}$$

$$\partial \tilde{p}_{j+4} / \partial z = \tfrac{1}{2} \partial^2 \tilde{w}_j / \partial \xi^2. \tag{3.25}$$

By eliminating $\tilde{u}_{j+4}$ and $\tilde{p}_{j+4}$ from (3.22)–(3.25), we obtain

$$\tfrac{1}{2} \partial^3 \tilde{v}_j / \partial \xi^3 + \partial \tilde{w}_j / \partial z = 0, \tag{3.26}$$

$$\partial \tilde{v}_j / \partial z = \tfrac{1}{2} \partial^3 \tilde{w}_j / \partial \xi^3. \tag{3.27}$$

Elimination of $\tilde{v}_j$ then yields

$$\partial^6 \tilde{w}_j / \partial \xi^6 + 4 \partial^2 \tilde{w}_j / \partial z^2 = 0. \tag{3.28}$$

The Ekman compatibility conditions

$$\tilde{w} = \mp \tfrac{1}{2} E^{\frac{1}{2}} \partial \tilde{v} / \partial \xi \quad \text{at} \quad z = \pm 1 \tag{3.29}$$

give us $\tilde{w}_j = 0$ ($j = 0$ and 1) at $z = \pm 1$. The solutions $\tilde{w}_0$ and $\tilde{w}_1$ of (3.28) which satisfy these conditions and tend to zero as $|\xi| \to \infty$ are identically zero in the $E^{\frac{1}{3}}$-layer. Because of this, (3.27) and (3.28) give us

$$\tilde{v}_j = a_j + b_j \xi + c_j \xi^2 \quad \text{for } j = 0 \text{ and } 1, \tag{3.30}$$

where a_j, b_j and c_j are functions of θ and t to be determined from matching conditions. Matching the solutions in the $E^{\frac{1}{3}}$-layer and in the $E^{\frac{1}{4}}$-layer yields the following conditions:

$$[\hat{v}_0]_- = a_0 = [\hat{v}_0]_+, \tag{3.31}$$

$$b_0 = 0, \quad c_0 = 0, \tag{3.32), (3.33}$$

$$[\hat{v}_1]_- = a_1 = [\hat{v}_1]_+, \tag{3.34}$$

$$[\partial \hat{v}_0 / \partial \eta]_- = b_1 = [\partial \hat{v}_0 / \partial \eta]_+ \tag{3.35}$$

and

$$c_1 = 0. \tag{3.36}$$

The equations for $\tilde{u}_6$, $\tilde{v}_2$, $\tilde{w}_2$ and $\tilde{p}_6$ are

$$\frac{\partial \tilde{u}_6}{\partial \xi} + \frac{1}{\gamma} \frac{\partial \tilde{v}_2}{\partial \theta} + \frac{\partial \tilde{w}_2}{\partial z} = 0, \tag{3.37}$$

$$\tilde{v}_2 = \partial \tilde{p}_6 / \partial \xi, \tag{3.38}$$

$$\frac{\partial \tilde{v}_0}{\partial t} + \frac{\beta}{\gamma} \hat{V}_0 \frac{\partial \tilde{v}_0}{\partial \theta} + \beta \frac{\partial \tilde{V}_1}{\partial \xi} \tilde{u}_3 + \tilde{u}_6 = -\frac{1}{\gamma} \frac{\partial \tilde{p}_6}{\partial \theta} + \frac{1}{2} \frac{\partial^2 \tilde{v}_2}{\partial \xi^2}, \tag{3.39}$$

$$\partial \tilde{p}_6 / \partial z = \tfrac{1}{2} \partial^2 \tilde{w}_2 / \partial \xi^2, \tag{3.40}$$

where we have used $\tilde{u}_0 = \tilde{u}_1 = \tilde{u}_2 = \tilde{p}_2 = \tilde{w}_0 = 0$. Because $\tilde{V}_0 = 0$ and $\tilde{V}_1 = \xi$ from (2.6), the first three terms on the left-hand side of (3.39) are independent of ξ. Therefore elimination of $\tilde{u}_6$ and $\tilde{p}_6$ from (3.37)–(3.40) gives us the same set of equations as (3.26) and (3.27) for $\tilde{v}_2$ and $\tilde{w}_2$. By following the same procedure as above, we obtain

$$\tilde{w}_2 = 0, \quad \tilde{v}_2 = a_2 + b_2\xi + c_2\xi^2, \tag{3.41), (3.42}$$

where a_2, b_2 and c_2 are functions of θ and t. The corresponding matching conditions are

$$[\hat{v}_2]_- = a_2 = [\hat{v}_2]_+, \tag{3.43}$$

$$[\partial\hat{v}_1/\partial\eta]_- = b_2 = [\partial\hat{v}_1/\partial\eta]_+ \tag{3.44}$$

and

$$[\partial^2\hat{v}_0/\partial\eta^2]_- = c_2 = [\partial^2\hat{v}_0/\partial\eta^2]_+. \tag{3.45}$$

The matching conditions (3.21), (3.31), (3.35) and (3.45) give us conditions on $\hat{\chi}_3$ at $\eta = 0$:

$$[\hat{\chi}_3]_- = [\hat{\chi}_3]_+, \quad \left[\frac{d\hat{\chi}_3}{d\eta}\right]_- = \left[\frac{d\hat{\chi}_3}{d\eta}\right]_+, \quad \left[\frac{d^2\hat{\chi}_3}{d\eta^2}\right]_- = \left[\frac{d^2\hat{\chi}_3}{d\eta^2}\right]_+, \quad \left[\frac{d^2\hat{\chi}_3}{d\eta^3}\right]_- = \left[\frac{d^3\hat{\chi}_3}{d\eta^3}\right]_+. \tag{3.46}$$

Substituting solutions hitherto obtained into (3.46), and dropping all the terms except the first three in (3.19), we obtain the dispersion equation

$$-64 - 144(\mu+\alpha) - 224(\mu^2+\alpha^2) - 16(\mu+\alpha)(5\mu^2 - \mu\alpha + 5\alpha^2) - 4(\mu^4 + 14\mu^2\alpha^2 + \alpha^4) + (\mu+\alpha)(\mu-\alpha)^2(3\mu^2 - 2\mu\alpha + 3\alpha^2) - (\mu^2+\alpha^2)(\mu^2-\alpha^2)^2 = 0, \tag{3.47}$$

where

$$\mu^2 = -2(i\omega - \tfrac{1}{2} + im\beta/\gamma) \tag{3.48}$$

and

$$\alpha^2 = -2(i\omega - \tfrac{1}{2} - im\beta/\gamma). \tag{3.49}$$

Because it is prohibitively difficult to get an explicit form of dispersion equation taking into account further terms in (3.19), we have not tried it. The coefficients in (3.47) are all real, therefore the complex-conjugate pair (μ^*, α^*) satisfies (3.47) if (μ, α) does. Consequently, if ω and $im\beta/\gamma$ are eigenvalues, their complex conjugates ω^* and $-im\beta/\gamma$ are also eigenvalues. This fact holds not only for (3.47) but also for the general form of the dispersion equation. As mentioned in the previous section, the dispersion equation in the case in which the inner plates rotate faster than the outer plates is obtained by replacing β by $-\beta$ in (3.47). Thus the eigenvalues in this case are ω^* and $+im\beta/\gamma$. Another thing to be noted is the similarity rule by which the dispersion equation is governed by a single parameter $m\beta/\gamma$. The disturbance is unstable if this parameter exceeds 9·5. This is demonstrated in figure 2, which shows ω_i *vs.* $2m\beta/\gamma$ according to (3.47).

4. The inviscid region

In this section we investigate the perturbations in the inviscid region and verify the assumptions made in §3: that $\hat{u}_0$, $\hat{u}_1$, $\hat{u}_2$, $\hat{p}_0$, $\hat{p}_1$, $\hat{p}_2$ and $\hat{v}_0$ tend to zero as $|\eta| \to \infty$.

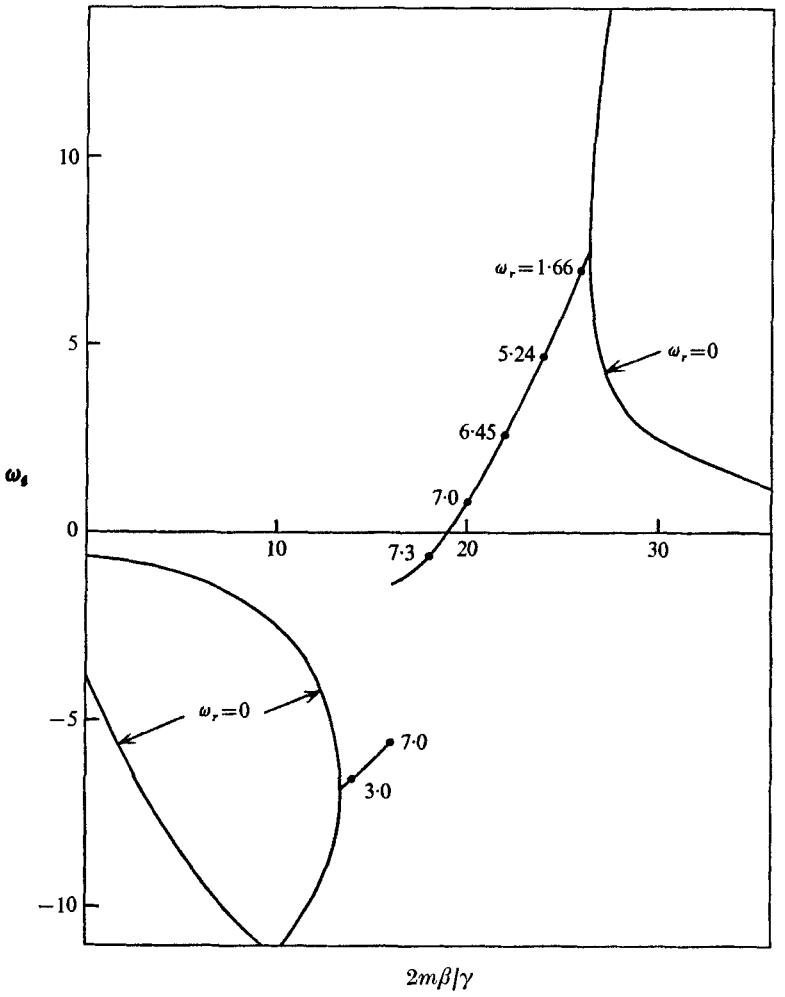

FIGURE 2. Stability diagram showing the growth rate ω_i *vs.* $2m\beta/\gamma$.

The inviscid region was treated by Busse for a general basic velocity distribution. Here we apply his results to our basic flow (2.4). The equations for $\mathbf{q}_j$ and p_j ($j = 0$, 1 and 2) are

$$\nabla.\mathbf{q}_j = 0, \quad \mathbf{k}\times\mathbf{q}_j = -\nabla p_j, \quad \nabla.\mathbf{q}_{j+6} = 0, \tag{4.1)–(4.3}$$

$$\partial\mathbf{q}_j/\partial t + \beta[(\mathbf{U}_0.\nabla)\mathbf{q}_j + (\mathbf{q}_j.\nabla)\mathbf{U}_0] + \mathbf{k}\times\mathbf{q}_{j+6} = -\nabla p_{j+6}. \tag{4.4}$$

From (4.1), (4.2) and the Ekman compatibility conditions (2.3), we obtain

$$w_j = 0, \quad v_j = -\partial p_j/\partial r, \quad u_j = -r^{-1}\partial p_j/\partial\theta. \tag{4.5}$$

If we assume p_j to be of the form

$$p_j = \mathrm{Re}\,[\chi_j(r)\exp\{i(m\theta - \omega t)\}], \tag{4.6}$$

for $j = 0$, 1 and 2, combination of (4.3)–(4.5) and (2.3) gives us

$$\frac{d^2\chi_j}{dr^2} + \frac{1}{r}\frac{d\chi_j}{dr} - \frac{m^2}{r^2}\chi_j = 0, \tag{4.7}$$

where use has been made of the fact that the basic flow is a rigid-body rotation. The solutions of (4.7) in the inner and outer inviscid regions are

$$\chi_j = \begin{cases} c_j r^m, & 0 \leqslant r < \gamma, \qquad (4.8) \\ c_j' r^m + c_j'' r^{-m}, & \gamma < r, \qquad (4.9) \end{cases}$$

where c_j, c_j' and c_j'' are constants. Because $\hat{u}_{j\eta} = \hat{p}_{j\eta} = \hat{u}_{j\xi} = \hat{p}_{j\xi}$ in the Stewartson layer for $j = 0$, 1 and 2, χ_j and $d\chi_j/dr$ must be continuous at $r = \gamma$. When there is a side wall at $r = r_w > \gamma$, the boundary condition on this side wall is $u_j = 0$, that is $\chi_j = 0$ at $r = r_w$. These three conditions combined with (4.8) and (4.9) give us $\chi_j = 0$ in the inviscid region. If there is no side wall, the first term r^m in (4.9) is omitted. Again the solution $\chi_j = 0$ results from the first two conditions. The fact that $\chi_j = 0$ in the inviscid region proves the self-consistency of the assumptions made in § 3.

5. Energy equations

Let us consider the energy balance for the disturbance. The largest magnitude of the disturbance velocity is of order $E^{\frac{1}{4}}$ in the inviscid region and of order unity in the $E^{\frac{1}{4}}$-layer and the $E^{\frac{1}{3}}$-layer. Thus the total kinetic energy of the disturbance is of order $E^{\frac{1}{2}}$ in the inviscid region, of order $E^{\frac{1}{4}}$ in the $E^{\frac{1}{4}}$-layer and of order $E^{\frac{1}{3}}$ in the $E^{\frac{1}{3}}$-layer. Therefore we can restrict ourselves to the $E^{\frac{1}{4}}$-layer. Multiplication of (3.9) by $\hat{v}_0$ and integration with respect to η over the $E^{\frac{1}{4}}$-layer gives us the energy equation of the disturbance:

$$\int_0^{2\pi} d\theta \int_{-\infty}^{\infty} d\eta \left\{ \frac{1}{2}\frac{\partial \hat{v}_0^2}{\partial t} + \beta \frac{d\hat{V}_0}{d\eta}\hat{u}_3\hat{v}_0 + \frac{\beta}{\gamma}\hat{V}_0\frac{\partial \hat{v}_0}{\partial \theta}\hat{v}_0 + \left(\hat{u}_6 + \frac{1}{\gamma}\frac{\partial \hat{p}_6}{\partial \theta} - \frac{\eta}{\gamma^2}\frac{\partial \hat{p}_3}{\partial \theta}\right)\hat{v}_0 - \frac{1}{2}\frac{\partial^2 \hat{v}_0}{\partial \eta^2}v_0 \right\} = 0, \qquad (5.1)$$

where integration with respect to z is not necessary because each term in (3.9) is independent of z. By performing partial integration and using (3.7), (3.8) and (3.10), we obtain the simpler expression

$$\frac{d}{dt}\int_{-\infty}^{\infty} \tfrac{1}{2}\overline{\hat{v}_0^2}\, d\eta = -\beta \int_{-\infty}^{\infty} \frac{d\hat{V}_0}{d\eta}\overline{\hat{u}_3\hat{v}_0}\, d\eta - \frac{1}{2}\int_{-\infty}^{\infty} \overline{\hat{v}_0^2}\, d\eta - \frac{1}{2}\int_{-\infty}^{\infty} \overline{\left(\frac{\partial \hat{v}_0}{\partial \eta}\right)^2}\, d\eta, \qquad (5.2)$$

where bars over letters indicate the average with respect to θ. The first, second and third terms on the right-hand side of (5.2) are the contributions from the main shear flow, the viscous dissipation in the Ekman layers and the viscous dissipation in the $E^{\frac{1}{4}}$-layer, respectively. In terms of $\hat{\chi}_3$, (5.2) becomes

$$\frac{d}{dt}\int_{-\infty}^{\infty} \tfrac{1}{2}\overline{\hat{v}_0^2}\, d\eta = -\frac{\pi m}{\gamma}\beta e^{2\omega_i t}\int_{-\infty}^{\infty} \frac{d\hat{V}_0}{d\eta}(\hat{\chi}_{3R}'\hat{\chi}_{3I} - \hat{\chi}_{3R}\hat{\chi}_{3I}')\, d\eta - \frac{\pi}{2}e^{2\omega_i t}\int_{-\infty}^{\infty}(\hat{\chi}_{3R}'^2 + \hat{\chi}_{3I}'^2)\, d\eta - \frac{\pi}{2}e^{2\omega_i t}\int_{-\infty}^{\infty}(\hat{\chi}_{3R}''^2 + \hat{\chi}_{3I}''^2)\, d\eta, \qquad (5.3)$$

where the subscripts R and I denote the real and the imaginary parts of $\hat{\chi}_3$, respectively, and the primes indicate differentiation with respect to η. Figure 3

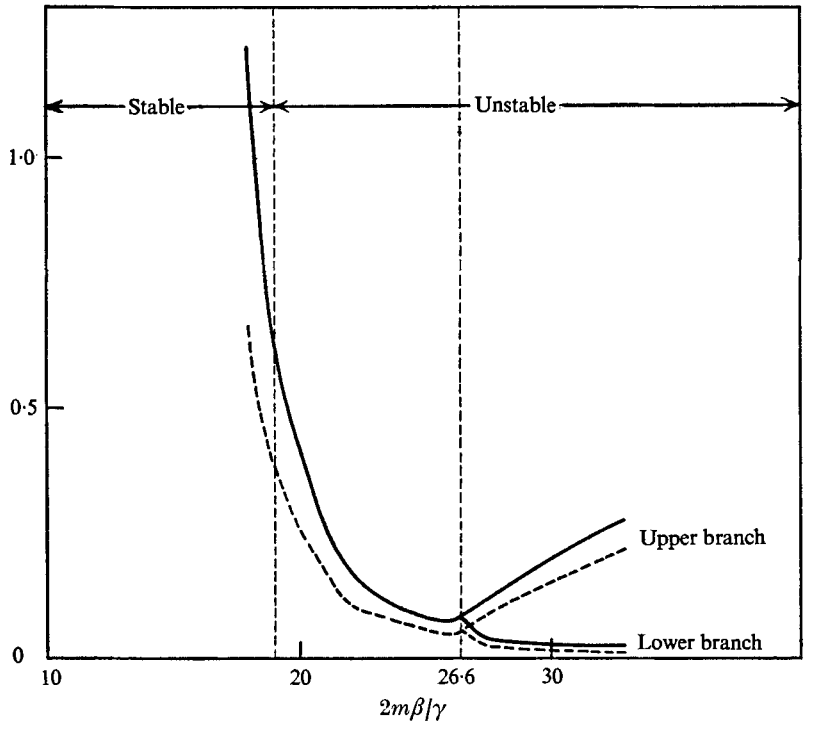

FIGURE 3. The ratios of the viscous dissipation terms in the $E^{\frac{1}{4}}$-layer (the third term on the right-hand side of (5.2); solid curves) and in the Ekman layer (the second term; dashed curves) to the energy contribution from the main flow (the third term) as functions of $2m\beta/\gamma$. For $2m\beta/\gamma > 26{\cdot}6$, ω_i has two possible values. Here the upper branch corresponds to the larger value of ω_i while the lower branch corresponds to the smaller value of ω_i.

gives the relative contributions of each dissipative term in comparison with that of the main shear flow. Figure 4 gives distribution in η space of each integrand on the right-hand side of (5.3) for a case of instability: $2m\beta/\gamma = 20$.

6. Concluding remarks

As we noted at the end of § 3, we have a similarity law by which the parameters m, γ and β in the dispersion equation combine to form the single parameter $m\beta/\gamma$. The Stewartson layer becomes unstable for $2m\beta/\gamma > 19$. To compare our results with the experimental data of Hide & Titman, we must take into account the fact that their Rossby number ϵ_{HT} and Ekman number E_{HT} are different from our Ro and E. Using the velocity distribution of the steady flow, we take $\frac{1}{2}d'$ as our characteristic length H and $\frac{1}{4}\Omega_1 + \frac{3}{4}\Omega_0$ (i.e. $\frac{1}{2}[\frac{1}{2}(\Omega_1 + \Omega_0) + \Omega_0]$) as our angular velocity Ω, where d' is the distance between the lower surface of the disk and the bottom of the tank, and Ω_0 and Ω_1 the angular velocities of the tank and the disk, respectively, in Hide & Titman's experiment (see figure 1). This gives

$$Ro = \gamma\epsilon_{HT}/2(4-\epsilon_{HT}), \quad E = 4\gamma^2 E_{HT}/(4-\epsilon_{HT}). \tag{6.1}$$

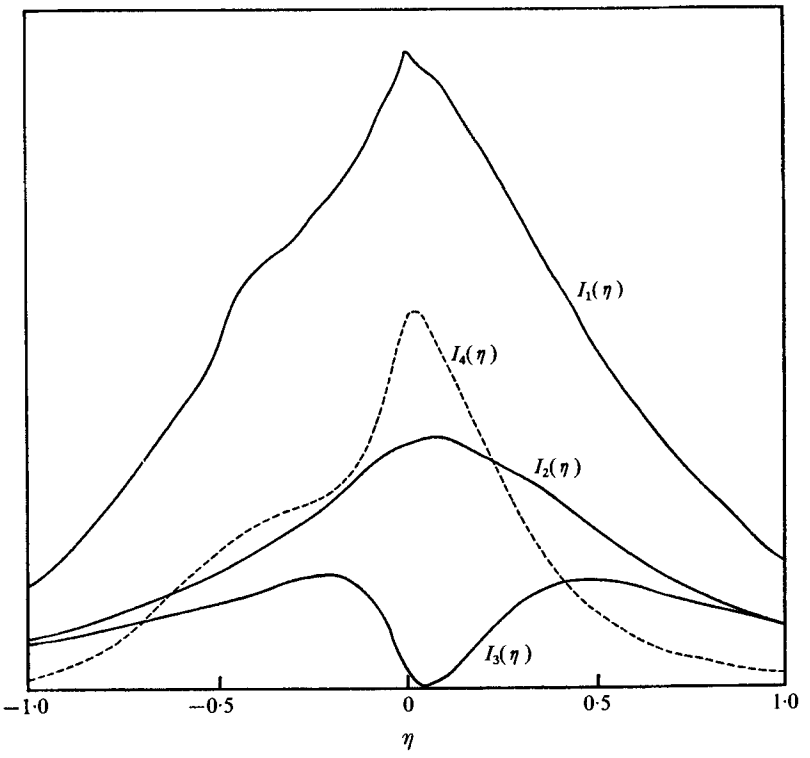

FIGURE 4. The distributions in η space of each integrand on the right-hand side of (5.3) for a case of instability: $2m\beta/\gamma = 20$. Here $I_1(\eta) = 2m\gamma^{-1}\beta\hat{V}_0'(\hat{\chi}'_{3R}\hat{\chi}_{3I} - \hat{\chi}_{3R}\hat{\chi}'_{3I})$, $I_2(\eta) = \hat{\chi}'^2_{3R} + \hat{\chi}'^2_{3I}$, $I_3(\eta) = \hat{\chi}^2_{3R} + \hat{\chi}^2_{3I}$ and $I_4(\eta) = I_1(\eta) - I_2(\eta) - I_3(\eta)$.

Combining these, we get

$$\frac{2m}{\gamma}\beta = \frac{m\epsilon_{HT}}{2\gamma[E_{HT}(4-\epsilon_{HT})]^{\frac{1}{2}}} \doteq \frac{m\epsilon_{HT}}{4\gamma E_{HT}^{\frac{1}{2}}}. \tag{6.2}$$

Our critical relation $2m\beta/\gamma = 19$ thus corresponds to the following relation between ϵ_{HT} and E_{HT}:

$$\log_{10}\epsilon_{HT} = \log_{10} 76\gamma/m - 0{\cdot}5\log_{10} E_{HT}^{-1}. \tag{6.3}$$

From table A1 in the Hide & Titman's paper, which gives experimental data determining the critical relation between ϵ_{HT} and E_{HT}, we can see that $\log_{10} 76\gamma/m$ is within the range

$$0{\cdot}76 \leqslant \log_{10} 76\gamma/m \leqslant 1{\cdot}16. \tag{6.4}$$

Relation (6.3) subject to (6.4) agrees well with the empirical relation given by Hide & Titman:

$$\log_{10}\epsilon_{HT} = 1{\cdot}225 \pm 0{\cdot}055 - (0{\cdot}586 \pm 0{\cdot}013)\log_{10} E_{HT}^{-1}. \tag{6.5}$$

Tables 1 and 2 give the values of $2m\beta/\gamma$ calculated from the experimental data of Hide & Titman, who observed the instability in 127 different situations. Figure 5 shows the observed frequency distribution of instabilities *vs.* $2m\beta/\gamma$ to

a (cm)	$E_{HT}^{-1} \times 10^{-3}$	ϵ_{HT}	m	β	$2\beta/\gamma$	$2m\beta/\gamma$
2·5	2·24	0·218	2	1·33	11·67	23·34
	3·58	0·184	2	1·41	12·40	24·80
	5·2	0·125	2	1·14	10·07	20·15
	7·11	0·104	3	1·11	9·77	29·32
	8·46	0·082	3	0·95	8·38	25·15
3·75	5·17	0·127	2	1·16	6·81	13·61
	7·7	0·109	3	1·21	7·11	21·34
	11·30	0·083	3	1·11	6·54	19·62
	15·7	0·074	3	1·17	6·86	20·59
	18·8	0·063	4	1·09	6·39	25·54
5·00	8·37	0·095	3	1·10	4·84	14·51
	13·4	0·073	3	1·07	4·69	14·07
	17·6	0·063	4	1·05	4·63	18·53
	27·7	0·053	4	1·11	4·88	19·54
	34·0	0·045	5	1·04	4·59	22·95
6·25	13·5	0·077	3	1·13	3·97	11·92
	21·2	0·059	4	1·08	3·81	15·23
	31·4	0·046	5	1·02	3·61	18·04
	43·0	0·039	5	1·02	3·58	17·88
	51·6	0·035	5	1·00	3·51	17·57
7·5	21·7	0·058	4	1·08	3·16	12·62
	30·2	0·038	5	0·83	2·43	12·16
	44·5	0·039	5	1·03	3·03	15·16
	61·7	0·032	6	1·00	2·93	17·56
	74·5	0·028	6	0·96	2·81	16·87

TABLE 1. All the β, $2\beta/\gamma$ and $2m\beta/\gamma$ determined from the experimental data in table A 1 of Hide & Titman.

give a clear view of the correspondence between our result and the experiment. We see that most of the instabilities observed lie in our unstable region. We may conclude, on the one hand, that the present theory explains why disturbances with wavenumber smaller than a certain critical value m^* were not observed experimentally. From the stability diagram in figure 2, on the other hand, the larger the wavenumber m, the larger is the growth rate. In the experiment, disturbances with wavenumber larger than a certain threshold value did not appear. The same discrepancy arises also in Siegmann's theory, in which ω_i increases in proportion to $(m^2-1)^{\frac{1}{2}}$. In relation to this point, Busse concluded that the wavelength of the most unstable mode is of the same order of magnitude as the shear-layer width. He obtained this result, however, in the limit of an infinitesimally thin shear layer. Because his theory becomes invalid in this limit, his conclusion must be re-examined. For example, we must take into account the effect of derivatives with respect to the azimuthal variable in the viscous terms of the basic equations.

No disturbance with $m = 1$ was observed in the experiment. According to Busse and Siegmann, this disturbance is stable regardless of the values Ro and E. Our result shows that this disturbance can be unstable when $\beta/\gamma > 9{\cdot}5$. Thus the

a (cm)	$E_{HT}^{-1} \times 10^{-3}$	ϵ_{HT}	m	β	$2\beta/\gamma$	$2m\beta/\gamma$
2·5	5·55	0·139	2	1·32	11·59	23·19
	5·6	0·157	2	1·50	13·19	26·37
	8·58	0·113	3	1·33	11·68	35·04
	8·67	0·133	2	1·57	13·85	27·71
	8·76	0·150	2	1·79	15·74	31·48
3·75	7·86	0·111	3	1·25	7·32	21·96
	7·95	0·129	2 (3)	1·46	8·57	17·15
	8·00	0·136	2 (3)	1·55	9·08	18·15
	8·05	0·149	2	1·70	9·99	19·98
	8·10	0·161	2	1·85	10·85	21·69
	10·80	0·112	3	1·48	8·66	25·97
	10·82	0·115	3?	1·52	8·90	26·70
	10·83	0·117	2 (3)	1·54	9·06	18·12
	10·95	0·137	2	1·82	10·70	21·40
	12·2	0·089	3	1·24	7·29	21·87
	12·3	0·098	3	1·38	8·07	24·21
	12·4	0·112	3	1·58	9·28	27·83
	12·5	0·128	2 (3)	1·82	10·67	21·33
	12·6	0·142	2	2·03	11·90	23·80
	19·1	0·0735	3?	1·28	7·52	22·56
	19·2	0·083	3	1·45	8·52	25·57
	19·25	0·090	3	1·58	9·26	27·79
	19·35	0·0975	3	1·72	10·07	30·21
	19·4	0·102	3	1·80	10·55	31·66
	19·5	0·1125	3	1·99	11·69	35·06
	19·6	0·1205	2 (3)	2·14	12·56	25·12
	19·7	0·129	2	2·30	13·50	26·99
5·00	13·5	0·0795	3	1·17	5·13	15·39
	13·6	0·0915	3	1·35	5·94	17·81
	13·8	0·121	3	1·80	7·94	23·82
	13·85	0·126	2 (3)	1·88	8·29	16·57
	14·05	0·149	2	2·25	9·90	19·80
	20·5	0·084	3	1·52	6·69	20·06
	20·6	0·095	3	1·72	7·59	22·77
	20·7	0·102	3	1·86	8·18	24·53
	20·8	0·104	3	1·90	8·36	25·08
	21·0	0·113	3	2·08	9·14	27·41
	21·1	0·118	2 (3)	2·17	9·57	19·14
	21·2	0·129	2 (3)	2·39	10·50	21·00
	21·3	0·138	2	2·56	11·27	22·55
	21·4	0·152	2	2·83	12·47	24·94
	27·1	0·053	4	1·10	4·83	19·32
	27·2	0·057	4	1·18	5·21	20·83
	27·25	0·0635	4	1·32	5·81	23·25
	27·4	0·0752	3	1·57	6·91	20·73
	27·5	0·0855	3	1·79	7·88	23·65
	27·6	0·0885	3	1·86	8·18	24·53
	27·8	0·102	3	2·15	9·48	28·43
	28·0	0·114	3	2·42	10·64	31·93
	28·1	0·125	2 (3)	2·66	11·71	23·42
	28·3	0·138	2 (3)	2·95	12·99	25·99
	28·5	0·148	2	3·18	14·00	28·01

[Table 2 continued on next page]

a (cm)	$E_{HT}^{-1} \times 10^{-3}$	ϵ_{HT}	m	β	$2\beta/\gamma$	$2m\beta/\gamma$
	34·5	0·0503	5	1·18	5·17	25·86
	34·9	0·0593	4	1·40	6·14	24·55
	35·0	0·0675	3 (4)	1·59	7·00	21·01
	35·0	0·068	3	1·60	7·06	21·17
	35·1	0·076	3	1·80	7·91	23·72
	35·5	0·094	3	2·24	9·86	29·57
	35·6	0·098	3	2·34	10·30	30·89
	35·8	0·112	3	2·69	11·82	35·47
	35·9	0·1175	2 (3)	2·82	12·43	24·86
	36·1	0·1275	2 (3)	3·08	13·54	27·08
	36·2	0·1315	2	3·18	13·99	27·99
	36·4	0·141	2	3·42	15·06	30·13
6·25	17·25	0·078	3	1·29	4·55	13·66
	17·35	0·088	3	1·47	5·16	15·47
	17·4	0·095	3	1·59	5·58	16·74
	17·55	0·1085	3	1·82	6·41	19·24
	17·7	0·129	3	2·18	7·68	23·03
	17·85	0·142	2	2·41	8·50	17·00
	43·1	0·0441	5	1·15	4·05	20·25
	43·8	0·0507	4	1·33	4·70	18·79
	44·0	0·061	4	1·61	5·67	22·69
	44·1	0·0669	3 (4)	1·77	6·23	18·70
	44·3	0·0752	3	2·00	7·03	21·09
	44·5	0·0908	3	2·42	8·53	25·58
	44·8	0·0985	3	2·64	9·29	27·87
	45·1	0·1095	3	2·95	10·37	31·12
	45·2	0·116	3	3·13	11·01	33·04
	45·6	0·132	2	3·58	12·61	25·22
7·50	62·0	0·048	5	1·50	4·41	22·04
	62·1	0·0515	4 (5)	1·61	4·74	18·95
	62·5	0·0625	4	1·97	5·77	23·10
	62·7	0·0677	4	2·14	6·27	25·08
	62·8	0·0695	3 (4)	2·20	6·44	19·33
	63·3	0·0837	3	2·66	7·80	23·41
	63·7	0·0971	3	3·10	9·10	27·29
	64·4	0·122	2 (3)	3·93	11·53	23·06
	64·6	0·1295	2 (3)	4·18	12·27	24·54
	64·9	0·136	2	4·41	12·93	25·85
	76·6	0·0295	6	1·02	3·00	18·03
	77·0	0·0345	5	1·20	3·53	17·63
	77·1	0·0418	5	1·46	4·28	21·39
	77·5	0·0532	4	1·86	5·47	21·87
	78·0	0·0652	4	2·29	6·73	26·93
	78·1	0·0662	3 (4)	2·33	6·84	20·52
	78·4	0·0707	3	2·50	7·32	21·97
	78·8	0·0775	3	2·75	8·06	24·17
	79·3	0·0905	3	3·22	9·45	28·36
	79·5	0·1035	3	3·70	10·84	32·52
	80·1	0·118	3	4·24	12·43	37·29
	81·2	0·1395	2	5·06	14·84	29·67

TABLE 2. All the β, $2\beta/\gamma$ and $2m\beta/\gamma$ determined from the experimental data in table A 2 of Hide & Titman

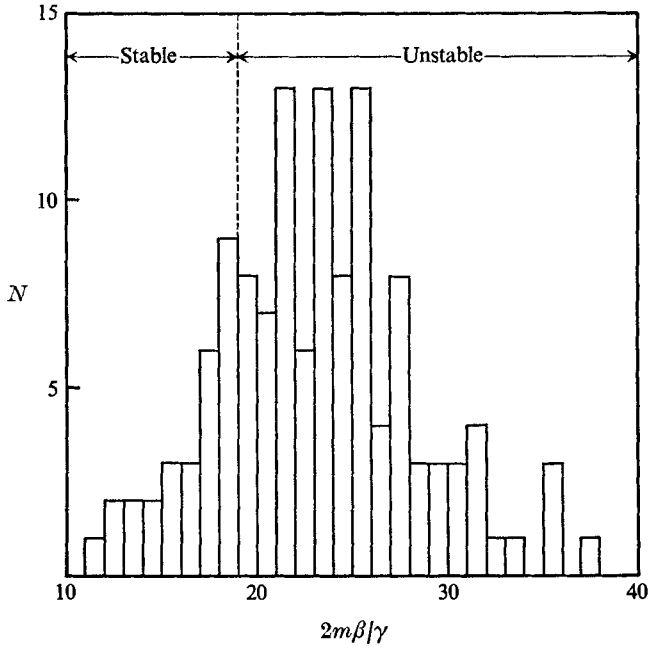

FIGURE 5. The observed instability frequency N *vs.* $2m\beta/\gamma$ on the basis of the experimental data of Hide & Titman.

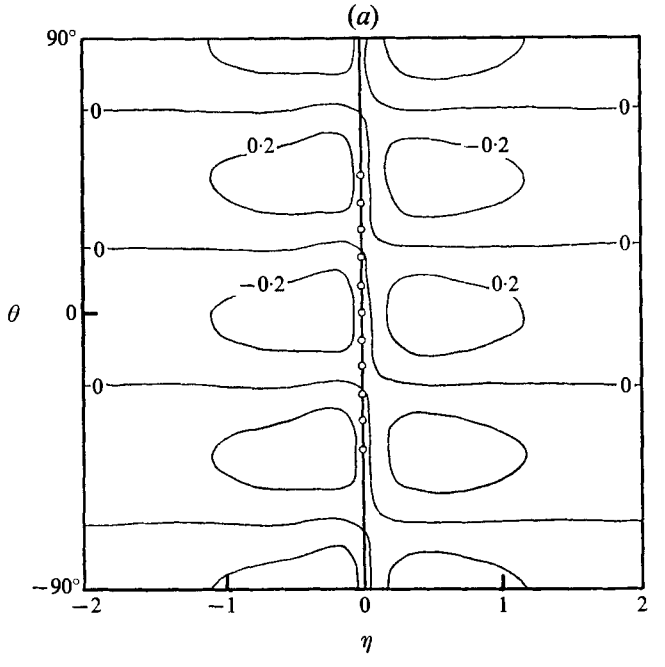

FIGURE (6*a*). For legend see page 305.

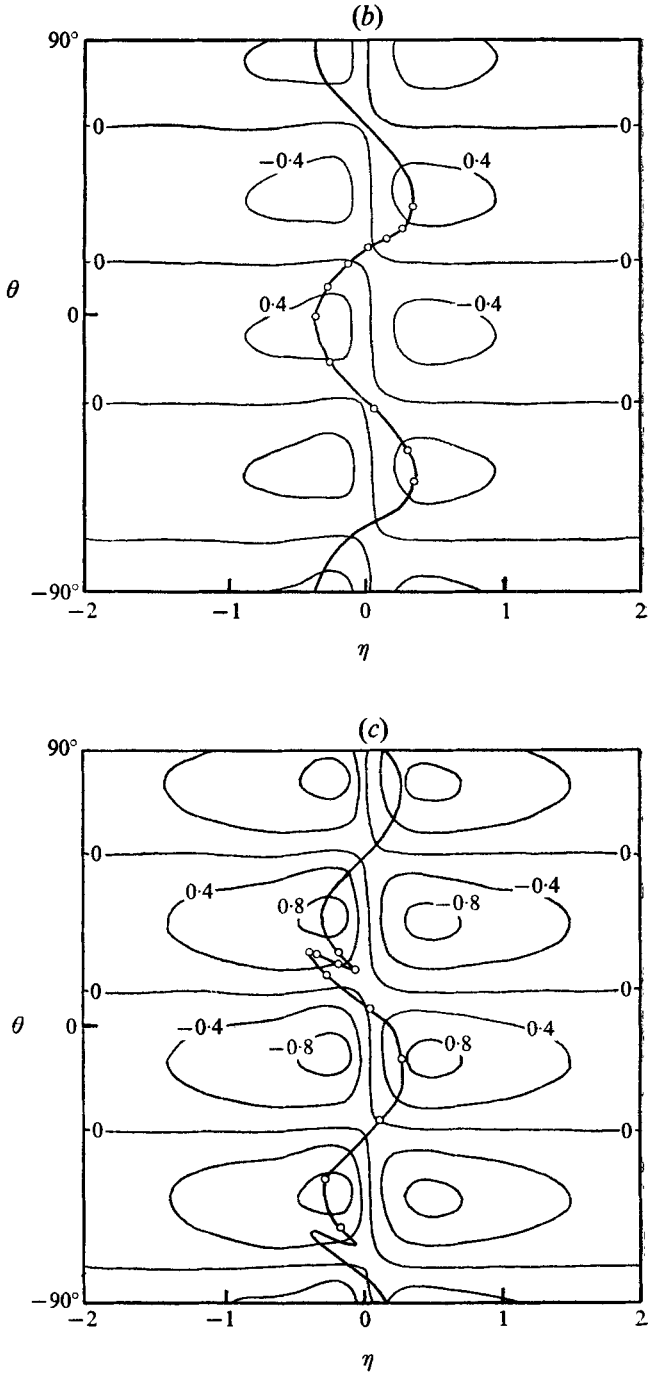

FIGURES 6(*b*, *c*). For legend see facing page.

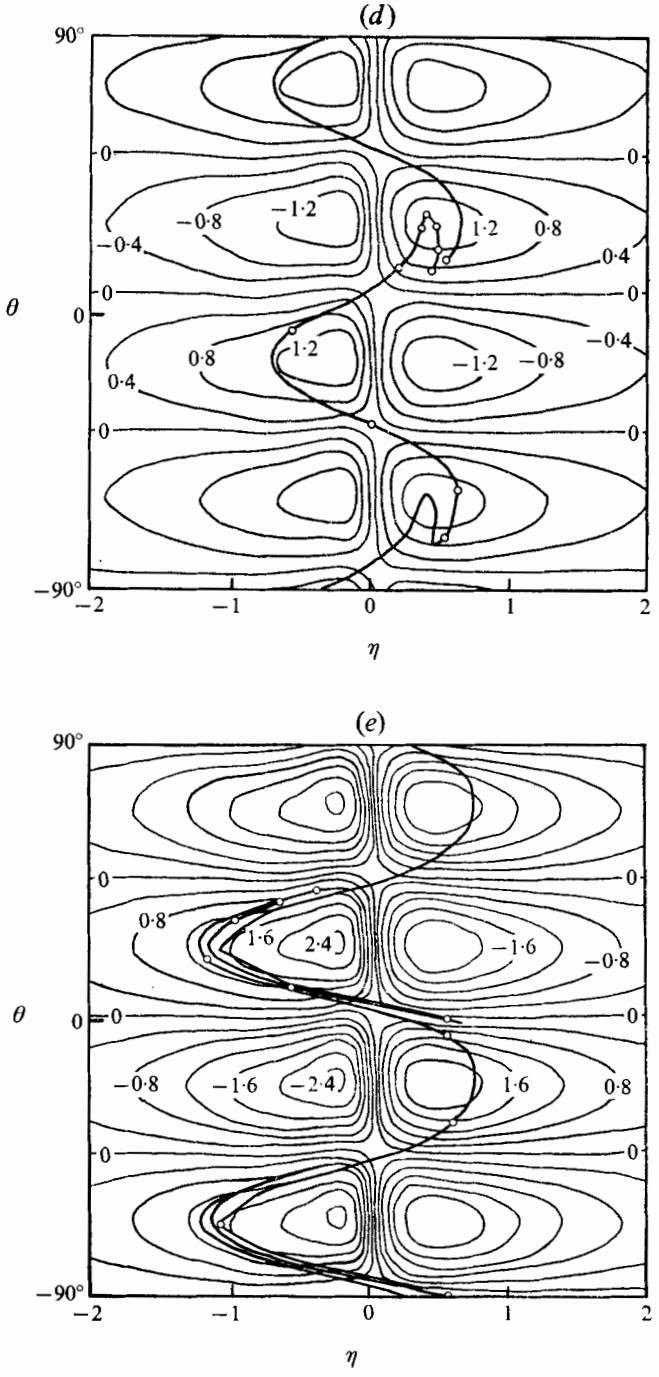

FIGURE 6. Distortion with time of a line of particles in the $E^{\frac{1}{4}}$-layer for the case $\omega_i = 1$, $\omega_r = -6{\cdot}98$, $\gamma = 1$, $m = 4$ and $\beta = -2{\cdot}5$. Equi-vorticity lines of the disturbance are also drawn. (*a*) $t = 0$. (*b*) $t = 0{\cdot}5$. (*c*) $t = 1{\cdot}0$. (*d*) $t = 1{\cdot}5$. (*e*) $t = 2{\cdot}0$.

only thing we can say is that the disturbance with $m = 1$ is stable in the parameter range of Hide & Titman's experiment (see table 1).

An interesting phenomenon observed in the experiment is the asymmetry of the flow with respect to the sign of the angular-velocity difference between the disk and the tank. As mentioned at the end of § 3, the solutions of the dispersion equation are symmetric with respect to the sign of the angular-velocity difference. The observed asymmetry may be explained by a nonlinear effect. Hide & Titman noted that certain details of the flow structure in the corner region, in which the free shear layer meets the Ekman layers, plays an important role in this asymmetry.

We must mention that the details of the velocity distribution in the Stewartson layer in the experiment are different from those in this paper. In the experiment, the Stewartson layer was generated by differential rotation of a disk in a cylindrical tank. There thus existed an axial flow from one side of the disk to the other through the corner region of the disk. This gave different matching conditions through the $E^{\frac{1}{3}}$-layer. From the theoretical point of view, we think it desirable to perform an experiment with the same configuration as that in this paper.

Finally, in figure 6, the time distortion of a line of particles in the $E^{\frac{1}{4}}$-layer is given. At an initial instant, uniformly spaced particles are aligned along the line $\eta = 0$. We can see a gradual folding up of this line of particles around the vorticity centre of the disturbance.

The author wishes to thank Professor Takeo Sakurai for his critical discussion of the manuscript. The numerical calculations were performed on the FACOM 230-60 electronic computer of the Data Processing Centre of Kyoto University.

REFERENCES

Busse, F. H. 1968 Shear flow instabilities in rotating systems. *J. Fluid Mech.* **33**, 577.

Greenspan, H. P. 1968 *The Theory of Rotating Fluids.* Cambridge University Press.

Hashimoto, K. 1975 A source-sink flow of an incompressible rotating fluid. *J. Phys. Soc. Japan*, **38**, 1508.

Hide, R. & Titman, C. W. 1967 Detached shear layers in a rotating fluid. *J. Fluid Mech.* **29**, 39.

Hunter, C. 1967 The axisymmetric flow in a rotating annulus due to a horizontally applied temperature gradient. *J. Fluid Mech.* **27**, 753.

Siegmann, W. L. 1974 Evolution of unstable shear layers in a rotating fluid. *J. Fluid Mech.* **64**, 289.

Stewartson, K. 1957 On almost rigid rotations. *J. Fluid Mech.* **3**, 17.